

# Full-F gyrofluid modelling of blob-impurity interaction in the tokamak scrape-off layer

E. Reiter<sup>1</sup>, M. Held<sup>1</sup>, A. Kendl<sup>1</sup>, M. Wiesenberger<sup>2</sup>

<sup>1</sup>Universität Innsbruck, Innsbruck, 6020, Austria

<sup>2</sup>Technical University of Denmark, Kongens Lyngby, 2800, Denmark

## Motivation: Impurity ions alter tokamak plasma evolution.

Impurities denote ions that are not part of the intended reactor fusion cycle, but are inevitably present in the plasma: Operating a tokamak involves plasma-wall interaction, intended at strike zones on divertor plates while undesirable anywhere else. Subjected to further ionisation, a significant number of sputtered wall particles will propagate into and severely disturb the plasma [1].

- ▶ **Negative effects** on tokamak performance stem from impurity accumulation **at the plasma core**, resulting in increased radiation losses (high mass impurities) and plasma dilution (low mass impurities) [2].
- ▶ **Beneficial effects** are expected from heat mitigation via impurity seeding **at the divertor** [3].

## Question: Impurities alter blob evolution?

Dependent on their concentrations, masses, charges and temperatures in a magnetised fusion plasma, **how do non-fuel ions, i.e. impurities, modify the dynamics of blobs** propagating through the scrape-off layer?

Common approaches in modelling turbulent impurity ion transport do not provide toolsets suitable for parameter studies on impurity-blob interaction:

- ▶ Gyrokinetic simulations [6] remain computationally expensive, whereas
- ▶ computationally attractive models most often resort to a “trace-approximation” with impurities as passive test particles not altering plasma evolution.

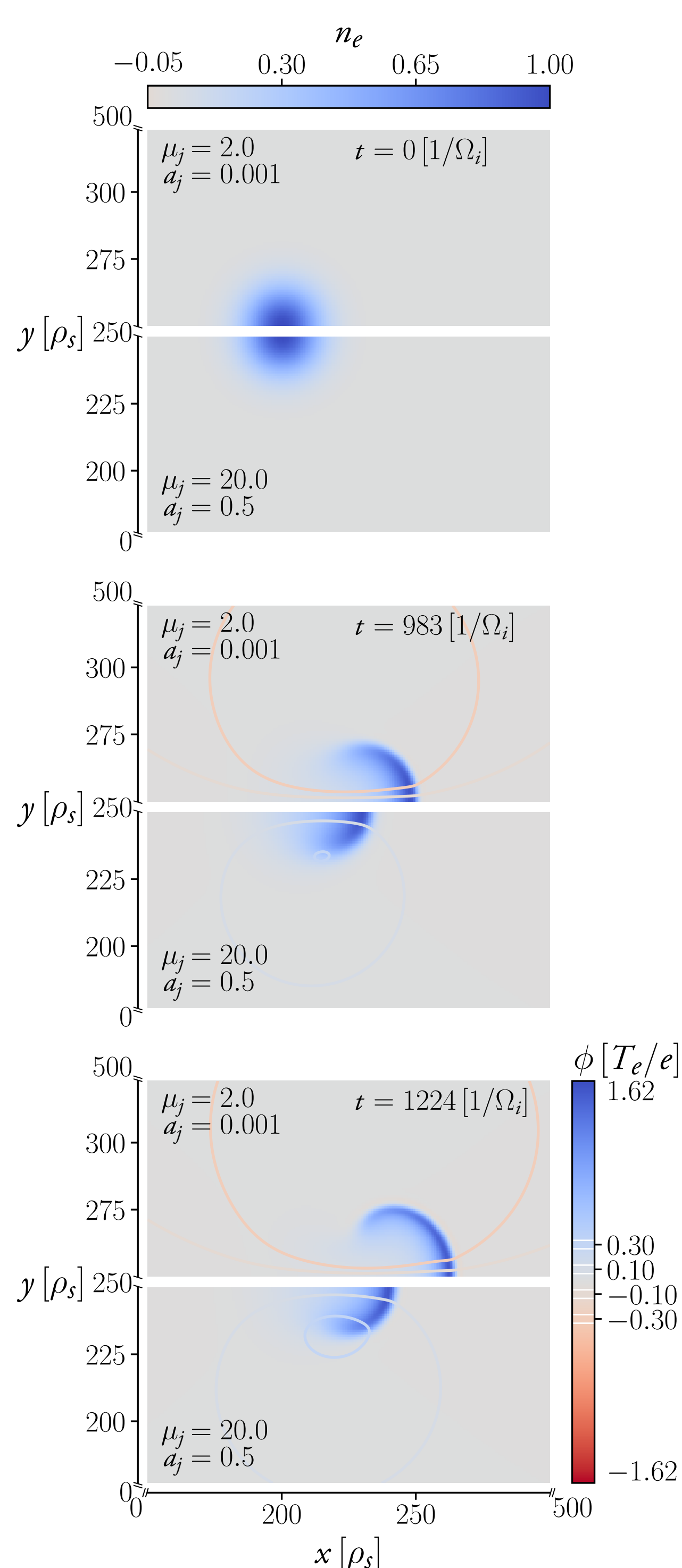


**Fig. 2:** Seeded cold fuel ion blob simulation with constant impurity background: Electron density  $n_e$  and electric potential  $\phi$ . Physical parameters resemble the SOL on the low field side of the ASDEX Upgrade tokamak (simulation parameters: Initial gaussian density distribution of fuel ions with amplitude  $\Delta n_i/n_i = 1$  and  $\sigma = 10$ , for  $\kappa = 0.000457$  and Reynolds number chosen to  $\mathcal{R}a = 10^9$ ).

## Data & licence



Sourcecode, scripts and parameters to reproduce simulations, results and this poster, available at:

<https://www.uibk.ac.at/ionen-angewandte-physik/comphys/efc17/efc17.html>

This poster is provided under a Creative Commons Attribution 4.0 International License.



## Result: Impurities slow blob propagation!

A parameter-scan on cold isothermal seeded blob simulations (initial fuel particle densities as Gaussian peaks with constant impurity background) for maximum perpendicular center-off-mass (COM) blob velocities (parameter proportional to heat and particle transport by the filaments) depicts:

- ▶ **Increased impurity concentration and/or higher mass-to-charge proportion of non-fuel ions results in slower blob propagation** (fig. 1) and hence less spatial dilation of the filament (compare fig. 2).
- ▶ Numerical experiments reproduce the analytical velocity scaling law for the set of full-F multi-species 2d gyrofluid equations.

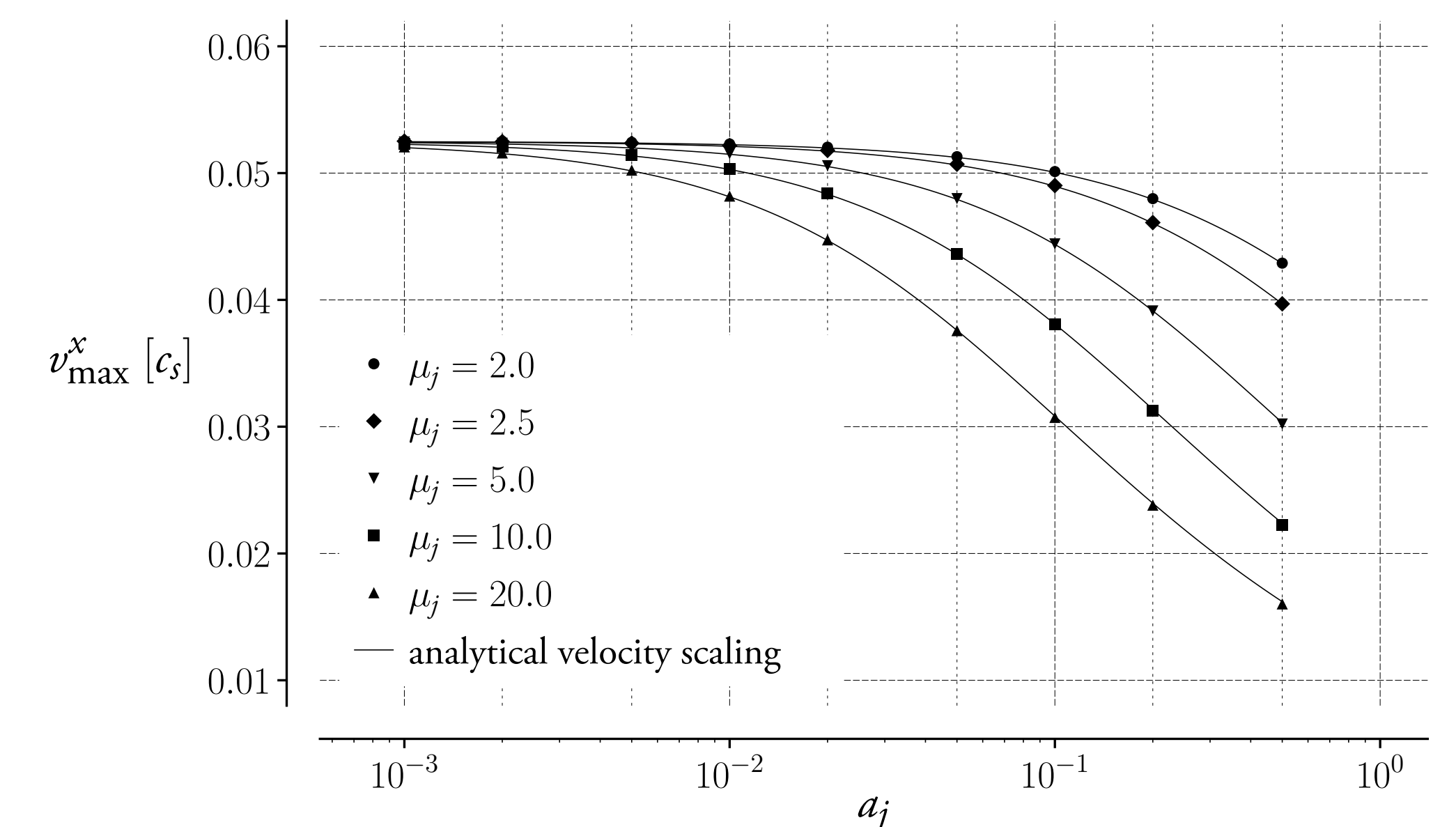


**Fig. 1:** Maximum perpendicular COM blob velocity  $v_{\max}^x$  (physical parameters resemble ASDEX-U low field side) dependent on impurity concentration  $a_j$  for different mass/charge proportions  $\mu_j$ .

## Model: Full-F multi-species 2d gyrofluid equations

The evolution of electron particle density  $n_e$  and ion gyrocenter densities  $N_s$  of fuel respectively impurity ions ( $s=i, j$ ) in a quasi-neutral, isothermal and electrostatic plasma is described via a full-F multi-species gyrofluid model. No distinction is made between dynamical background and fluctuations.

By gyro-Bohm normalisation (referencing ion gyrofrequency  $\Omega_i = eB_0/m_i$ , drift scale  $\rho_s = \sqrt{m_i T_e}/(eB_0)$  and cold ion acoustic speed  $c_s = \rho_s \Omega_i$ ) dimensionless equations are derived in an orthonormal 2D slab geometry. Dynamics parallel to  $\hat{z}$  direction are neglected, the magnetic field strength  $B$  varies radially alongside  $\hat{x}$  via  $1/B = (1 + x/R)/B_0$ , with  $R$  the major tokamak radius:

$$\begin{aligned} \partial_t n_e + \frac{1}{B} \{ \phi, n_e \} - n_e \kappa \partial_y \phi + \kappa \partial_y n_e &= -\nu \nabla_{\perp}^4 n_e \\ \partial_t N_s + \frac{1}{B} \{ \psi_s, N_s \} - N_s \kappa \partial_y \psi_s - \tau_s \kappa \partial_y N_s &= -\nu \nabla_{\perp}^4 N_s \\ \sum_s \left[ \nabla_{\perp} \cdot \left( \frac{a_s \mu_s N_s}{B^2} \nabla_{\perp} \phi \right) - n_e + a_s \Gamma_s N_s \right] &= 0 \end{aligned} \quad \begin{aligned} \Gamma_s &= \left( 1 - \frac{1}{2} \tau_s \mu_s \nabla_{\perp}^2 \right)^{-1} \dots \text{Padé approximation of gyroaveraging operator} \\ \psi_s &= \Gamma_s \phi - \frac{1}{2} \mu_s \left( \frac{\nabla_{\perp} \phi}{B} \right)^2 \dots \text{FLR corrected electric potential} \end{aligned}$$

With reference to fuel ion mass  $m_i$  and electron temperature  $T_e$  a set of three dimensionless parameters:

$$\mu_s = \frac{m_s}{Z_s m_i}, \quad \tau_s = \frac{T_s}{Z_s T_e} \quad \text{and} \quad a_s = \frac{Z_s n_{s,0}}{n_{e,0}}$$

accounts for charge numbers  $Z_s$ , masses  $m_s$ , temperatures  $T_s$  and concentrations of different ion species.

Poisson-Brackets  $\{, \}$  are used in denoting  $\mathbf{E} \times \mathbf{B}$  advection,  $\nabla_{\perp}$  abbreviates application of  $-\hat{z} \times (\hat{z} \times \nabla)$  and  $\kappa = 1/R$ . Fourth order hyperdiffusion  $-\nu \nabla_{\perp}^4$  ensures numerical stability.

## Model: Energy conservation

$$\begin{aligned} \partial_t \int d\Omega \left[ n_e \ln n_e + \sum_s a_s \tau_s N_s \ln N_s + \frac{1}{2} \sum_s a_s \mu_s N_s \left( \frac{\nabla_{\perp} \phi}{B^2} \right)^2 \right] &= \\ \nu \int d\Omega \left[ \nabla_{\perp}^4 n_e (1 + \ln n_e - \phi) + \sum_s a_s \nabla_{\perp}^4 N_s (\tau_s + \tau_s \ln N_s - \psi_s) \right] & \end{aligned}$$

## Method: FELTOR numerical library

The multi-species 2d gyrofluid equation set is integrated using the FELTOR C++ numerical library [7]:

- ▶ Discontinuous Galerkin spatial discretisation,
- ▶ semi-implicit multistep time integrator (Karniadakis),

both access a preconditioned conjugate gradient solver.

Calculations scale on distributed as well as on shared memory systems, efficiently executable on CPUs and GPUs (NVIDIA) as well as on accelerators (Intel Xeon Phi: Knights Landing).

## Outlook: Hot ions & impurity inhomogeneity

Model and method include multiple impurity species, finite ion temperatures and arbitrary initial impurity distributions (examples depicted in fig. 3). Further simulations will examine:

- ▶ temperature effects on impurity-blob interaction,
- ▶ Blob propagation/multi-species impurity transport with inhomogeneous particle distributions.

Comparison with gyrokinetic calculations for impurity transport by blobs and holes [6] will provide a useful benchmark.

## Preliminaries: Blobs dominate transport across the plasma edge.

At the edge of magnetised fusion plasmas **radially propagating filaments**, elongated along field-lines, **dominate heat and particle transport**. Fueled by steep pressure gradients at the vicinity of the last closed flux surface these “blobs” are expelled into the scrape-off layer (SOL).

- ▶ Particle density amplitudes of such perturbations compared to the background can be well above unity [4], defying any model based on separation of background and fluctuating quantities.
- ▶ The strong anisotropy of a tokamak magnetic field decouples perpendicular from parallel blob dynamics and scales (taking the  $\mathbf{B}$ -field orientation as a reference) [5].

## Model: Velocity scaling

Scaling analysis of the vorticity equation provides an equation for the growth rate  $\gamma$  and hence for the maximum perpendicular velocity of a  $\sigma$ -sized blob with amplitude  $A$ :

$$v_{\max}^x := \gamma \sigma \propto \sqrt{\frac{A \kappa \sigma (1 + \sum_s a_s \tau_s)}{\sum_s a_s \mu_s}}$$

## Model: Derivation

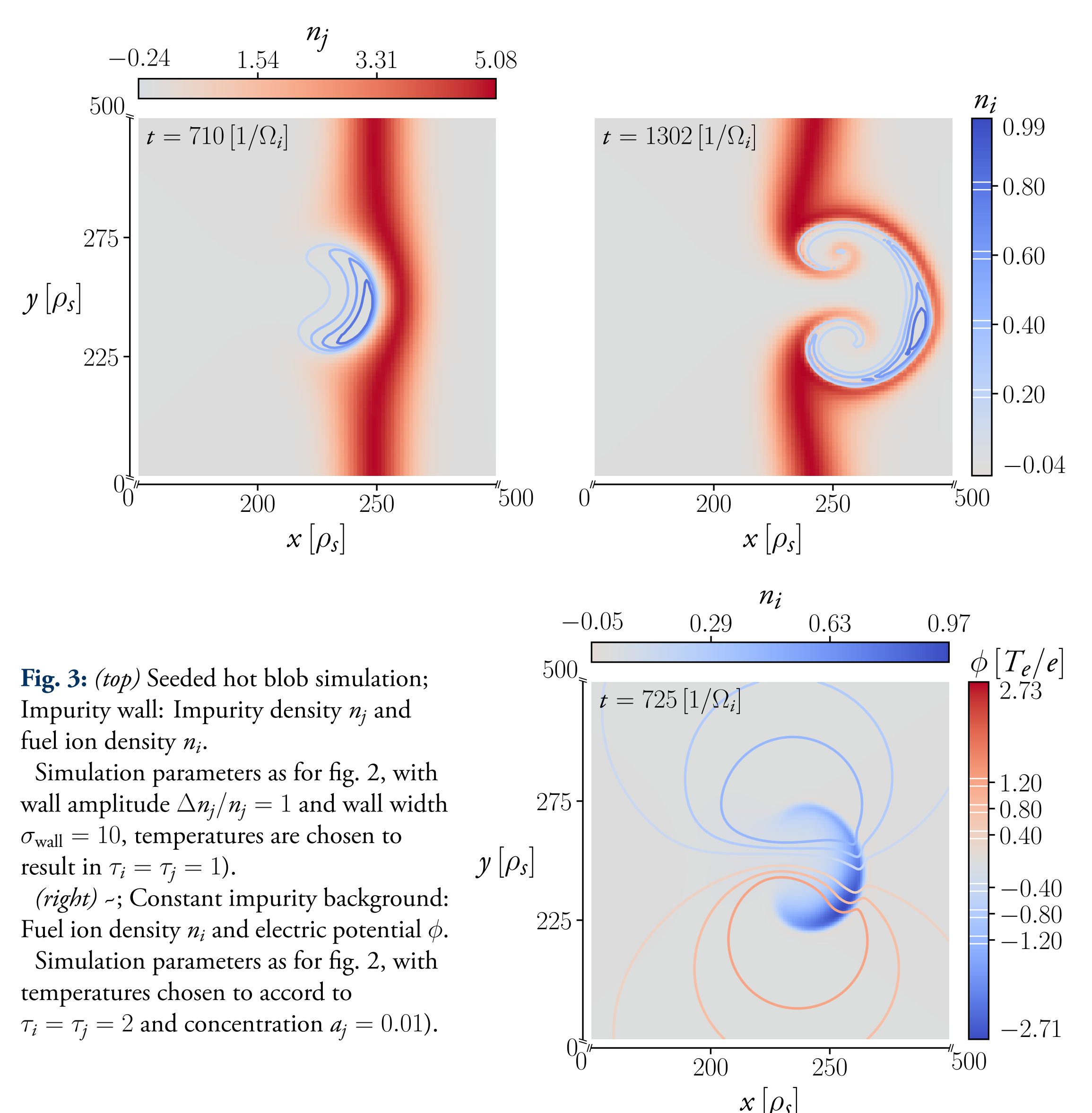
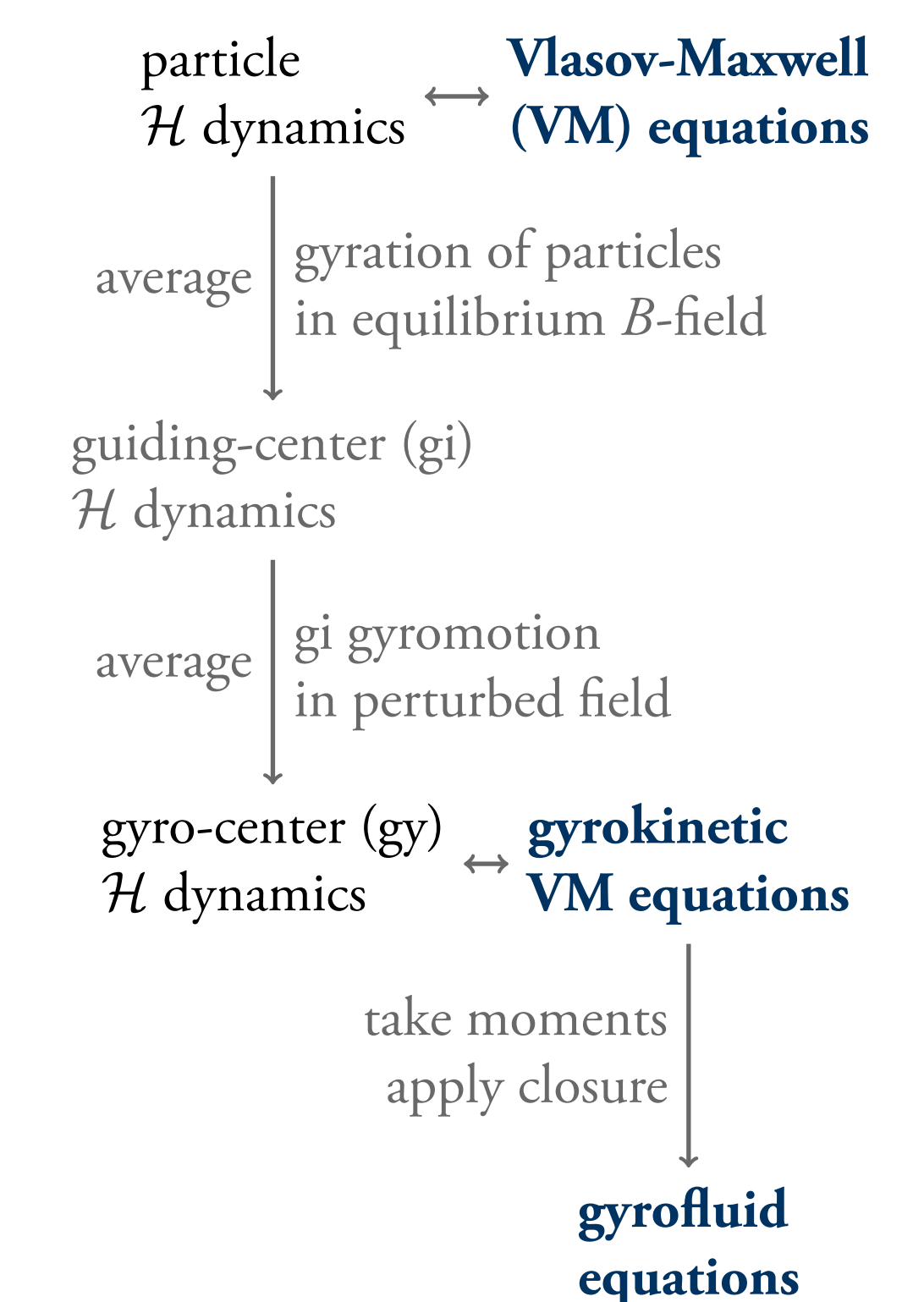


**Fig. 3:** (top) Seeded hot blob simulation; Impurity wall: Impurity density  $n_j$  and fuel ion density  $n_i$ . Simulation parameters as for fig. 2, with wall amplitude  $\Delta n_j/n_j = 1$  and wall width  $\sigma_{\text{wall}} = 10$ , temperatures are chosen to result in  $\tau_i = \tau_j = 1$ . (right) -; Constant impurity background: Fuel ion density  $n_i$  and electric potential  $\phi$ . Simulation parameters as for fig. 2, with temperatures chosen to accord to  $\tau_i = \tau_j = 2$  and concentration  $a_j = 0.01$ .

## Acknowledgements

This work is partly supported by the Austrian science fund (FWF) Y398. It has been carried out within the framework of the EUROfusion Consortium and has received funding from the Euratom research and training programme 2014-2018 under grant agreement No. 633053. The views and opinions expressed herein do not necessarily reflect those of the European Commission. Eduard Reiter acknowledges further support by an ÖAW KKKÖ Matching Grant. Computational results presented have been achieved (in part) using the Vienna Science Cluster (VSC2).

## References

- [1] A. Kendl, Int. J. Mass Spectrom. 365-366, 106–113 (2014)
- [2] C. Angioni et al., Phys. Plasmas 14, 055905 (2007)
- [3] D. Brunner et al., Nucl. Fusion 57, 086030 (2017)
- [4] S. Zweben et al., Nucl. Fusion 55, 093035 (2015)
- [5] M. Held et al., Nucl. Fusion 56, 126005 (2016)
- [6] H. Hasegawa and S. Ishiguro, Nucl. Fusion 57, 116051 (2017)
- [7] [github.com/feltor-dev/feltor](https://github.com/feltor-dev/feltor)